Toward Space-Air-Ground Integrated Network Simulation with 4D Topologies

Mario Franke and Christoph Sommer
TU Dresden, Faculty of Computer Science, Germany
https://www.cms-labs.org/people/{ franke , sommer }

***Abstract*—Future Space-Air-Ground Integrated Networks (SAGINs) involving Low Earth Orbit (LEO) satellites are characterized by a high degree of mobility in all of the space, the air, and the ground segment – leading to high in-segment and between-segment network topology dynamics. Mobility simulation in an integrated space and ground simulation model has thus been identified as one of the key challenges of future research. In this paper we demonstrate that such an integration can be achieved by picking a point in the center of the scenario, the Satellite Observer Position (SOP), and constructing an East-North-Up (ENU) tangential plane through it to arrive at an all-Cartesian coordinate system. Its construction is well-aligned with the needs of Vehicle-to-Satellite (V2S) between-segment channel modeling without sacrificing accuracy for in-segment communication – and which lends itself well to large-scale, high-efficiency simulation of future SAGINs. We back our assumptions with a detailed study on the potential impact of loss of accuracy, demonstrating it to be negligible for most practical purposes in the target application domain. We demonstrate the potential of the presented fully-integrated approach in a small proof-of-concept simulation study where we investigate the impact of small position differences of air/ground nodes in their interplay with the space segment.**

I. Introduction

Space-Air-Ground Integrated Network (SAGIN) system and protocol design and optimization is a research field that has changed dramatically in recent years: First, Vehicular networks are now a reality, also introducing mobility considerations on the ground, relative to not just fixed infrastructure but also to each other, to Unmanned Aerial Vehicles (UAVs), and to satellites. Second, Non-Terrestrial Networks (NTNs) for 5G and 6G space-to-ground connectivity are driving commoditization of satellite connectivity for ground nodes, massively increasing the scale of such networks. Third, massive and multi-shell Low Earth Orbit (LEO) satellite deployments in the *New Space* sector have brought relative mobility considerations in the space segment to the forefront of research.

Taken together, this means that modern SAGINs are now characterized by a high degree of mobility in all of the space, the air, and the ground segment – and that the mobility of nodes must be considered relative to each other. This leads to 3D network topologies that change rapidly, but also predictably, over time (cf. Figure 1) – meaning that nodes can not just exploit 3D topology information but can also exploit topology dynamics information: *4D topologies*.

A key challenge is, thus, to develop simulation models that can capture the complexity of such 4D topologies. Previous work has made progress in this direction, but has, so far, focused on either satellite or on air/ground node mobility [1], [2] – and work that uses separate simulations for the space, air, and ground segments cannot capture the challenges nor the opportunities arising from the interplay between the segments.

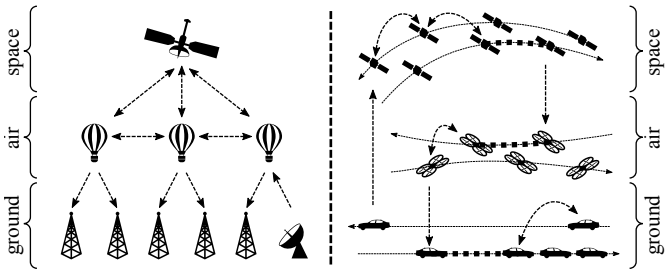

(a) traditional, low topology dynamics (b) high topology dynamics

Figure 1. Contrast between (a) traditional, low topology dynamic Space-Air-Ground Integrated Networks (SAGINs) and (b) more recent, high topology dynamic SAGINs. While (a) emphasizes classic routing and networking problems, (b) emphasizes speed and predictable mobility, also introducing aspects of opportunistic networking.

Indeed, current surveys on SAGIN designs [3] point to mobility as one of the key challenges of such systems. Moreover, current surveys on SAGIN simulation [4] point out that the first important future research direction is to move away from separate simulators and toward the integrated simulation of both the space and ground segments. While first solutions to overcome these challenges exist (as shown in Section II), they either oversimplify network topology dynamics due to the different scales of LEO satellite and air/ground node mobility – or they do not evaluate the errors introduced by their abstractions.

To fill this gap, this paper's contributions are: I) An efficient and fully integrated approach to SAGIN simulation which lends itself well to large-scale, high-efficiency simulation of future SAGINs. II) An in-depth investigation demonstrating its benefits in terms of accurate Vehicle-to-Satellite (V2S) between-segment channel modeling without sacrificing accuracy for Vehicle-to-Vehicle (V2V) or Satellite-to-Satellite (S2S) in-segment communication; as well as an investigation of limits of its applicability. III) A proof-of-concept simulation study showing the impact of small position differences of air/ground nodes in their interplay with the space segment. We also make a reference implementation of our approach available as open source, as part of our space_Veins simulator.

19th IEEE/IFIP Conference on Wireless On demand Network Systems and Services (WONS 2024) Digital library entry →
http://dx.doi.org/10.23919/WONS60642.2024.10449583

II. Related Work

Many simulators have been developed for Space-Air-Ground Integrated Network (SAGIN) research and many are excellent tools for their intended purpose, but most of them have been designed with a strong focus on only one or two of the three segments (space, air, or ground) of such a network, modeling the other segments only abstractly.

We categorize related work into four groups according to the level of detail with mobility is modeled in the space and ground segment.

Work in the first group bases results on abstract concepts of connectivity such as quasi-static connectivity [5], contact plans [6], stochastic geometry [7], or stochastic models [8].

Work in the second group models satellite mobility only very abstractly. Examples are work that employs fully-featured mobility models for cars while abstracting all satellites into one singular abstract entity with perfect connectivity [9], work that needs not model satellite mobility because they are assumed to be geostationary [10], and work where satellite mobility is modeled as linear movement in one direction at a fixed height [11].

Work in the third group focuses on modeling satellite mobility in detail, but abstracts from ground station mobility. Some of the work in this group performs mobility calculations using closed source simulators [12], [13] whereas most work utilizes models such as the Simplified General Perturbations 4 (SGP4) model or circular orbits based on Keplerian orbit elements [14]–[19]. Ground mobility, however, is static or highly abstract – that is, work in this group need not focus on coordinate transformations and the corresponding accuracy loss in ground mobility modeling.

Work in the fourth group is most closely related to our work: it considers both satellite and ground station mobility in detail. Puttonen et al. [20] evaluate 5G NTNs. Its satellite mobility is based on the SGP4 model and ground station mobility models support 3D fixed speed movements. Cheng et al. [21] go one step further and combine two closed-source simulators for satellite and vehicular mobility modeling. Both works, however, do not reveal details on the methods used to combine mobility models, their efficiency, nor which level of accuracy is achieved.

We can thus conclude that related work either does not consider mobility in one of the three segments (space, air, or ground), substitutes only abstract mobility models for one of the three segments, or does not reveal details on the chosen methods to combine mobility models, their efficiency, nor which level of accuracy is achieved.

We fill this gap by focusing on exactly this integration and discussing all three mentioned key aspects and the resulting accuracy trade-offs in detail. We present an approach (see Section III), discuss its end-to-end integration (with a reference implementation available as open source, see Section IV), all validated by an accuracy study described in Section V with claims substantiated by a proof-of-concept study presented in Section VI.

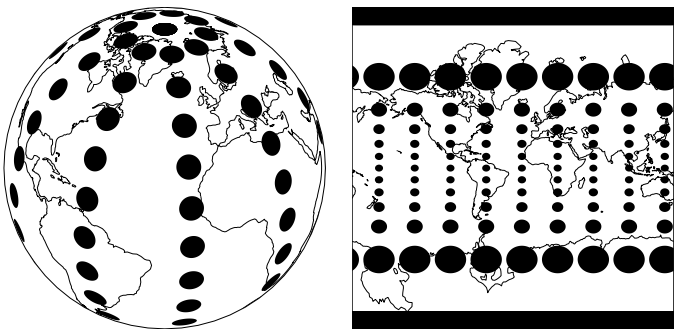

(a) *Orthographic* (*3D view*) (b) *Mercator* clipped to ±87° latitude

Figure 2. Illustration of the inability of map projections to preserve required geometric properties globally, shown for the example of (a) Orthographic and (b) Mercator projection: Equilongitudinal, equilatitudinal, and equally-sized discs (*Tissot's indicatrix*) appear entirely different in terms of horizontal and vertical distance in (b) – to the point where they deform from discs into bands at the poles.

III. Combining Coordinate Systems

Before we can discuss the concept of integrated Space-Air-Ground Integrated Network (SAGIN) simulation, we must first discuss approaches to combining the coordinate systems of LEO satellites and air/ground nodes. For the satellite coordinates, we build on an observer-centric concept as proposed by Franke et al. [22], which we briefly recap. We build on this concept to integrate air/ground node positions, move beyond the need for a separate LEO mobility simulator, discuss the benefits and investigate the drawbacks of this approach, and we present a proof-of-concept simulation study of an integrated SAGIN scenario.

While both LEO satellite and Vehicle-to-Everything (V2X) simulators model mobility and communication, the motion patterns of nodes differ in all of scale, speed, distance, and dimensionality. LEO satellite network simulators commonly use a spherical coordinate system, often decoupled from the Earth's rotation, allowing fast orbital calculations. Conversely, however, air/ground node mobility simulators such as the road traffic simulator *Eclipse SUMO* together with network simulation models contained in, e.g., *ns-3* or *Veins* [23] internally work with a Cartesian coordinate system describing the surface of Earth, commonly obtained via map projection, e.g., using Universal Transverse Mercator (UTM).

A first, obvious potential solution to the problem of combining the two coordinate systems is, therefore, to use a common *map projection* (e.g., using UTM) to project the ground trace of all LEO satellite positions onto a 2D plane and to employ each satellite's altitude above ground as its height above the plane. This has the salient benefits of allowing all model calculations to be performed in a single, unified coordinate system – and of this coordinate system being Cartesian, which makes for computationally-inexpensive geometrical calculations involving positions, speeds, and angles. These benefits, however, come at the cost of introducing substantial projection errors: Any simulation would need to choose between two similarly-bad alternatives: Either, it would use a map projection that is

valid for all of Earth, but very imprecise in the near field (causing large errors in air/ground node network topology calculation). Or, it would use a map projection that is precise enough for the region on Earth where air/ground node mobility should be investigated, but likely invalid for the region where many of the LEO satellites are located (causing large errors in relative satellite positions and, thus, satellite network topology calculation). More generally, any map projection will introduce errors in linear distances, angular distances, or areas, and these errors will vary with position, as illustrated in Figure 2. Both options are thus similarly unfit for fully-integrated SAGIN simulation with topology dynamic considerations in all three segments (space, air, and ground).

A second, equally straightforward solution is to inverse map project all air/ground node positions to spherical coordinates relative to an assumed center of Earth – and to then perform all model calculations in this coordinate system. This, however, would need all validated models to be partially re-implemented in spherical coordinates and to partially perform map-projection on the fly for each model calculation, which is not just computationally expensive but also error-prone and likely to cause cumulative errors at scale.

We thus build our simulation on a third solution, a Satellite Observer Position (SOP) centric approach. It is based on the observation that the most relevant measures for channel modeling between air/ground nodes and LEO satellites are the {azimuth angle, elevation angle, and distance} of each satellite relative to an air/ground node – as opposed to its {longitude, latitude, and altitude} tuple in a global coordinate system. Further, that these measures are somewhat similar for all air/ground nodes in a given scenario (an assumption whose impact we set out to validate in this paper). We thus choose a representative virtual air/ground node, the SOP, for each scenario – relative to which we transform all satellite positions into Cartesian coordinates. This approach aims to combine the advantages of being able to work in all-Cartesian coordinates with the advantages of closely preserving the aforementioned measures most relevant to channel modeling between LEO satellites and air/ground nodes. At the same time, it avoids the disadvantages that either of the alternative approaches (applying common map projections or working in spherical coordinates) would introduce. It also ensures that major directions (horizontal and vertical – east/north and up) are aligned with the axes of the coordinate system, easing model implementation and efficiency. We present an approach for integrated simulation based on this concept as well as an investigation of the validity of this approach in the following.

IV. Integrated Simulation

We build the fully integrated Space-Air-Ground Integrated Network (SAGIN) computer simulation on the models of the Veins [23] simulation framework for Connected Autonomous Vehicle (CAV) modeling and the INET Framework [24] for Internet protocol modeling. These, in turn, build on the OMNeT++ network simulator [25] and the SUMO road traffic simulator [26]. We extend the model libraries with simulation models of satellite mobility following a Satellite Observer Position (SOP) centric approach as described in Section III and make the resulting suite available in version 0.3 of our Open Source simulation framework *space_Veins*.[1]

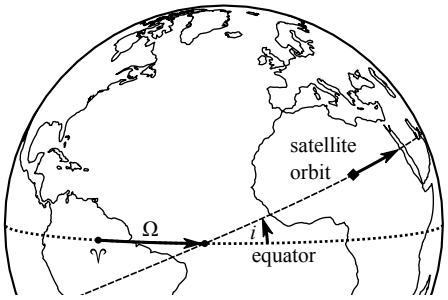

Figure 3. Illustration of $i = 25°$ and $\Omega = 30°$ as given in NASA/NORAD Two-line Element Set (TLE) data (here: if longitude −60° currently faces toward the *first point of aries* ♈).

```
1 25544U 98067A   08264.51782528 -.00002182  00000-0 -11606-4 0  2927
2 25544  51.6416 247.4627 0006703 130.5360 325.0288 15.72125391563537
```

Figure 4. Sample NASA/NORAD Two-line Element Set (TLE) data [27] for the International Space Station on a day in late 2008, encoding, e.g., an orbital inclination of $i = 51.6°$, a right ascension of the ascending node of $\Omega = 247°$, and a mean motion of $n = 15.7$ revolutions per day.

To be able to accurately model satellite mobility, we make use of publicly-available NASA/NORAD Two-line Element Set (TLE) data [28], which contains, for each satellite, its name, timestamp of record (*epoch time*), current angular position in orbit (as mean anomaly M), speed (as mean motion n) as well as its first and second time derivatives, and many other *orbital elements* (parameters) such as inclination i and right ascension of the ascending node Ω. See Figure 3 for an illustration of how these parameters define an orbit, Figure 4 for an example of TLE data. This data is sufficient to describe any valid orbit, quasi-circular or deformed, of a satellite close to Earth along with how it changes over time.

The SGP4 algorithm, as implemented by Vallado et al. [29] in the 2017-02-20 version of its companion code, is then applied to compute (*propagate*) future satellite positions in a True Equator Mean Equinox (TEME) Earth-Centered Inertial (ECI) coordinate system. As a first step towards a common coordinate system we then transform these to International Terrestrial Reference Frame (ITRF) Earth-Centered Earth-Fixed (ECEF) coordinates, that is, coordinates which rotate with Earth. From there, we can rely on the established *proj* library (version 8.2.1) to transform them to WGS84 coordinates, then, to geocentric Cartesian coordinates (x,y,z coordinates relative to the center of a round Earth – not to be confused with map projection to a flat representation of Earth; see Figure 5 for an illustration) and, then, topocentric Cartesian coordinates, specifically: East-North-Up (ENU) coordinates on a local tangent plane centered on the SOP. The ENU coordinates directly serve as the x, y, and z coordinates of satellites in the air/ground node simulation

[1]Full source code available via https://sat.car2x.org/

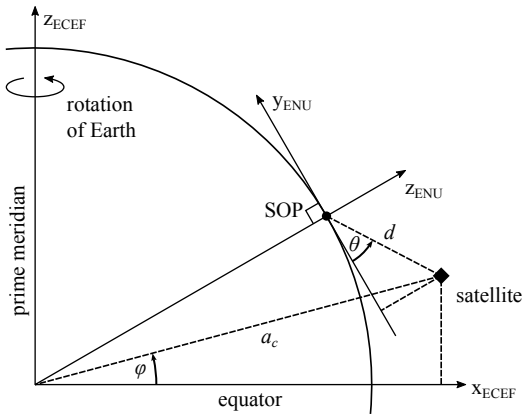

Figure 5. Equivalent coordinates in Earth-Centered Earth-Fixed (ECEF) latitude/altitude (φ/a_c), ECEF Cartesian ($x_{\text{ECEF}}/z_{\text{ECEF}}$), and East-North-Up (ENU) Cartesian ($y_{\text{ENU}}/z_{\text{ENU}}$) coordinates on a tangential plane. Also: Derived coordinates θ and d for Vehicle-to-Satellite (V2S) channel modeling.

fully integrating satellite and air/ground node positions in a shared, Cartesian coordinate system with $z = 0$ being the height of the ground.

It bears repeating that the described coordinate transformations on satellite positions necessary to arrive at a common Cartesian coordinate system did not involve any kind of common map projection (which would have introduced distortions in satellite positions and mobility). That said, (unlike the described *satellite* simulation) many air/ground node simulators internally *do* employ map projection to arrive at the Cartesian coordinates of, e.g., roads and buildings based on geodata. Here, however, distortions are kept manageable by the (comparatively very small) scale of such simulations, which allows for location-specific projection parameters (such as those defined for UTM zones) to be employed. Moreover, the actual mobility calculations of such simulators take place in Cartesian space, so (while, for bad projection parameters, a simulated road might well be slightly longer than in reality) the mobility patterns of air/ground nodes themselves, even on wrongly-projected roads, do not suffer from projection errors.

Knowing the relative location of satellites and air/ground nodes in a shared Cartesian coordinate system then allows to efficiently compute the elevation angle θ and distance d of any satellite relative to any air/ground node to be used for channel simulation. We use d to compute propagation delay and θ to determine satellite reachability by ensuring that θ exceeds a threshold θ_{lim}. Common values of θ_{lim} are physical limits (such as $0°$ to ensure that a satellite is visible above the horizon) or regulatory limits (such as the minimum elevation angle of $\theta_{\text{lim}} = 25°$ to be commonly observed by *SpaceX Starlink* satellites [30, III-E-1 para. 42]).

V. Accuracy Study

As a consequence of the design of the Satellite Observer Position (SOP) centric approach and its implementation in the integrated simulator, the accuracy of the simulation can be expected to depend on the distance of an air/ground node to the SOP. We set out to investigate the magnitude of this effect in the following.

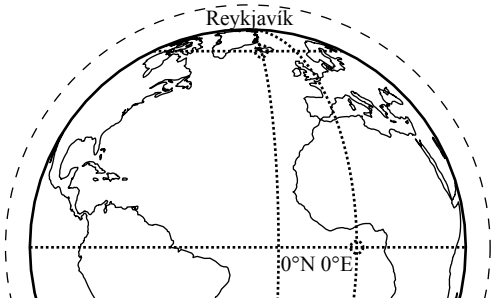

Figure 6. Size relations of scenario parameters: Midpoints of the two simulated scenarios, one at 0°N 0°E (*Null Island*) and one at 64.13°N −21.90°E (in Reykjavík, Iceland), where bands of longitude are visibly narrower. Also plotted is the maximum of all median orbit heights of the simulated Low Earth Orbit (LEO) satellites (dashed line), approx. 780 km above the Earth.

We select two scenarios, one at 0°N 0°E (*Null Island*) and one at approx. 64.13°N −21.90°E (in Reykjavík, Iceland), where bands of longitude are much narrower. In each scenario, we choose the SOP to be in the center. Figure 6 shows the size relations of the scenario parameters.

As point of comparison for the accuracy study, we employ the established *Skyfield* library [31] (version 1.46). With it, we calculate, for each pair of potential communication partners separately, the positions of the involved satellite in space and the involved air/ground node on the WGS84 reference ellipsoid, deriving the relative elevation angle θ and distance d of this pair. Unlike the coordinate transformations that we apply in our integrated simulation, this approach works in celestial coordinates and can thus yield higher precision for an individual V2S link – at the cost of potentially sacrificing precision for in-segment links. It also forgoes the computational benefits of the SOP centric approach, where all participants share a Cartesian coordinate system and geometry is predominantly axis aligned because it is relative to a tangential ENU plane, as discussed in Section III. However, it can serve as a point of comparison to investigate deviations between results obtained via the two approaches.

As the space segment of our scenarios, we simulate 80 satellites of the IRIDIUM NEXT constellation (IRIDIUM 102 through 181, with number 100 standing in for what would have been number 127). Of those, 67 are in orbit at an altitude of approx. 780 km (circling Earth approx. 14 times per day), the remainder at up to 150 km lower orbits (where, e.g., spare satellites are *stored* to fill coverage holes). All satellites are in orbits with mean inclinations of approx. 86.4°.

As the ground segment of our scenarios, we consider ground stations positioned along the positive x-axis, as we expect accuracy to drop with increasing longitude difference between the SOP and the ground station. Investigating realistic scenario widths, we find that common SUMO community scenarios [32] measure approximately in width: 2 km (*Bologna Pasubia* and *Acosta*), 4 km (*Bologna Ringway*), 10 km (*MoST Monaco*), and 14 km (*LuST Luxembourg*) – though newer scenarios are

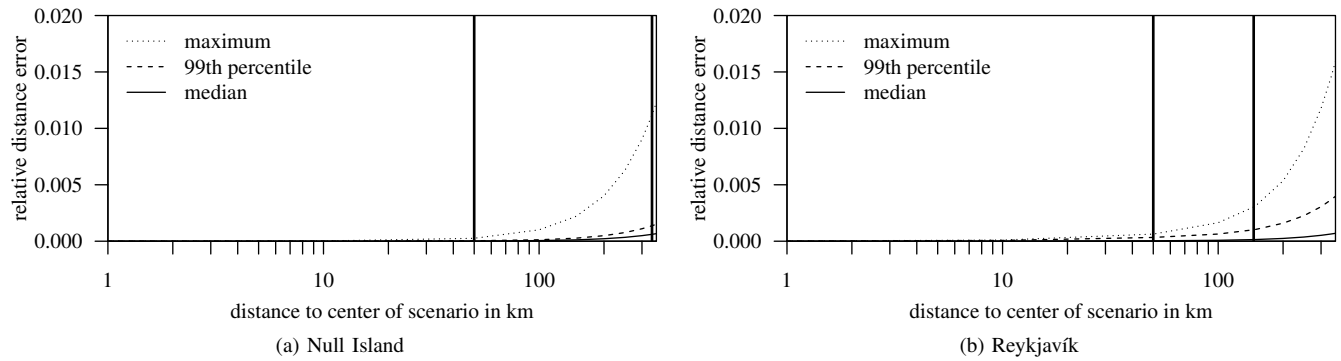

(a) Null Island (b) Reykjavík

Figure 7. Distance of a ground station to the center of the scenario vs. relative distance error (δd) of the satellite connection. Vertical lines mark 50 km (the maximum distance to the Satellite Observer Position, SOP, in a practical, 100 km wide scenario) as well as 146 km and 334 km in the *Null Island* and *Reykjavík* scenarios, respectively (the maximum distance to the SOP in a full 6° UTM zone at the latitude of the scenario).

becoming ever bigger: 25 km (*TuST Turin*), 32 km (*TAPAS Cologne*), 46 km (*BeST Berlin*), 68 km (*STOMP Stuttgart*). Nevertheless, for completeness, we investigate accuracy at distances from the SOP of up to 350 km, thus covering theoretical scenarios of more than the full width of an entire UTM zone of 6° (approx. 668 km at the equator) – far beyond the width of typical microscopic road traffic scenarios.

We simulate 12 hours of satellite mobility, checking connectivity for each satellite and ground station combination every second. For each, we investigate three metrics:

A. Relative Distance Error

As a first metric, we investigate the relative error incurred in predicting the distance d between a satellite and a ground station as a measure for, e.g., the error in computing propagation delay. We do this in both of the discussed locations, *Null Island* and *Reykjavík* to investigate the impact of the latitude of the investigated location, that is, of the curvature of Earth. We obtain one paired sample for each simulated transmission attempt between a satellite and a ground station by computing the distance obtained via our SOP centric approach relative to the corresponding distance obtained via Skyfield and taking the deviation from 100 % (a perfect match), that is,

$$\delta d = \left| 100\% - \frac{d_{\text{SOP}}}{d_{\text{Skyfield}}} \right| . \tag{1}$$

From this, we can calculate the median, 99$^{\text{th}}$ percentile, and maximum of δd for each simulated distance between ground station and SOP.

Figures 7a and 7b show the results of this investigation. The first result that sticks out is that the median and even the 99$^{\text{th}}$ percentile of the error δd is negligible for most practical purposes: below 0.40 % for all distances in both scenarios. It can also be seen that δd, especially its 99$^{\text{th}}$ percentile, is slightly higher in the *Reykjavík* scenario than in the *Null Island* scenario, which is to be expected as the curvature of Earth is more pronounced at higher latitudes.

Lastly, we see that, for practical scenario sizes of up to 100 km (corresponding to a maximum distance to the SOP of 50 km), even the maximum observed δd stays below 0.06 %. It is not until be we reach scenarios as wide as a whole 6° UTM zone (a maximum distance to the SOP of 334 km in the *Null Island* scenario and 146 km in the *Reykjavík* scenario) that we see the maximum δd reach 1.12 % and 0.30 %, respectively.

We can thus conclude that, for most practical purposes such as for propagation delay calculations, the SOP centric approach does not introduce any relevant error in the calculation of distance to the satellite d.

B. Elevation Error

As a second metric, we investigate the error in elevation angle θ as an indication of the stability of geometry calculations. Like when calculating the distance error δd, for every simulated transmission attempt between a satellite and a ground station, we collect one paired sample for Skyfield and our SOP centric approach. For this pair, we calculate the absolute difference, that is,

$$\Delta\theta = \left| \theta_{\text{SOP}} - \theta_{\text{Skyfield}} \right| . \tag{2}$$

Figures 8a and 8b show the results of this investigation. Here, we notice much more pronounced errors (as compared to the distance error δd) not just in the maximum and 99$^{\text{th}}$ percentile but also in the median: For practical scenario sizes of up to 100 km (corresponding to a maximum distance to the SOP of 50 km) the median $\Delta\theta$ now reaches 0.22° and 0.27° in the *Null Island* and *Reykjavík* scenarios, respectively.

The maximum $\Delta\theta$ for the same distance is even higher, reaching 0.46° and 0.46° in the *Null Island* and *Reykjavík* scenarios, respectively. Moving to scenarios as wide as a full 6° UTM zone we can see $\Delta\theta$ reaching as much as 3.43° and 1.40° in the *Null Island* and *Reykjavík* scenarios, respectively.

From this we can conclude that, other than the distance error δd, the elevation error $\Delta\theta$ (which informs decisions on whether communication with the satellite is viable according to a threshold θ_{lim}) cannot be dismissed outright, but a more detailed investigation is needed.

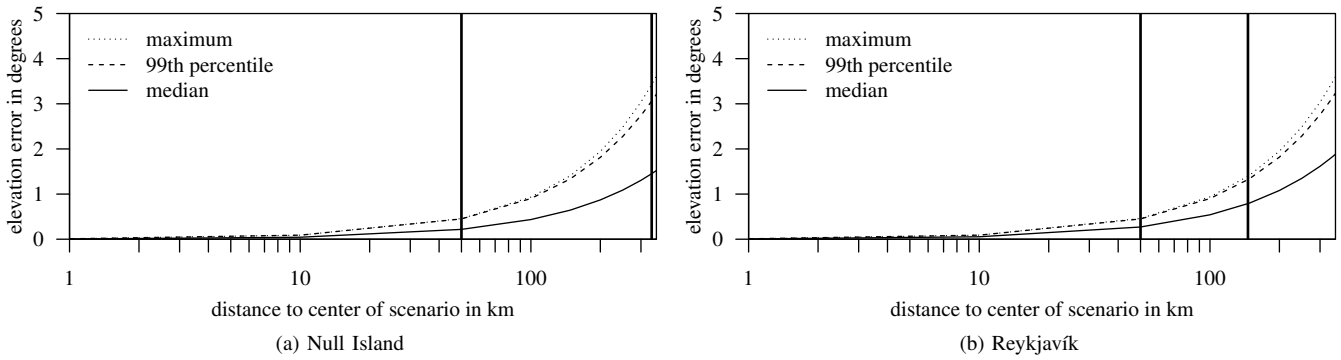

(a) Null Island (b) Reykjavík

Figure 8. Like Figure 7, but plotting the elevation error ($\Delta\theta$).

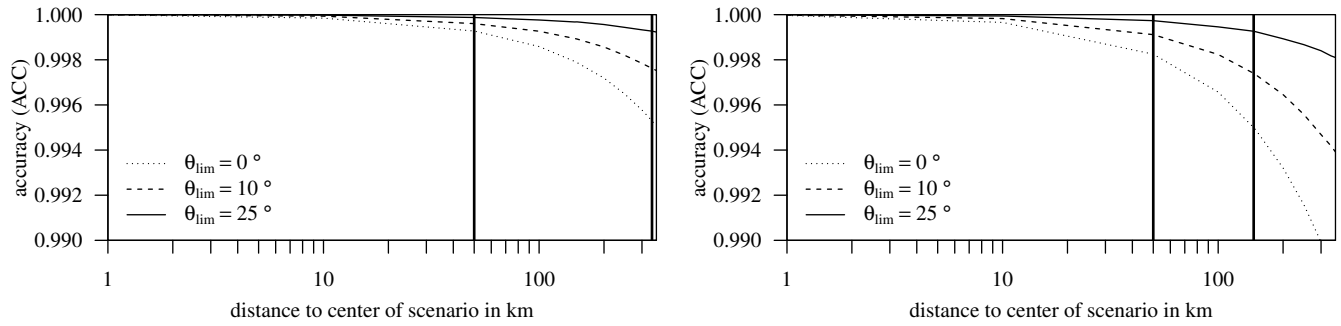

(a) Null Island (b) Reykjavík

Figure 9. Like Figures 7 and 8, but plotting the accuracy of connectivity prediction (ACC).

C. Accuracy

As a third metric, we therefore investigate a metric more directly tied to application performance: the accuracy achieved when predicting whether a connection between a satellite and a ground node is viable. As discussed, we consider a connection to be viable if the elevation angle θ exceeds a threshold θ_{lim}, starting at 25° (see Section IV) – though we also investigate 10° and 0°. By comparing predictions (on whether θ_{lim} was met) of Skyfield and our SOP centric approach, we can then compute the accuracy of the SOP centric approach in predicting connection viability. For this, we classify each of the total number m of viability predictions as *true* (either true positive or true negative – TP and TN, respectively) if they match and as *false* if they do not. This allows us to derive the classic accuracy metric

$$\text{ACC} = (\text{TP} + \text{TN})/m, \tag{3}$$

revealing which fraction of connectivity predictions is correct (in the sense of the two approaches agreeing).

Figures 9a and 9b show the results of this investigation, which put the previous results into perspective: As can be seen, distance to the SOP *does* have a noticeable effect on accuracy – to some degree in the *Null Island* scenario and somewhat stronger in the *Reykjavík* scenario where the curvature of Earth is more pronounced. However, the effect of distance on the accuracy (ACC) is smaller than the investigation of $\Delta\theta$ might have suggested: Even in scenarios as wide as a full 6° UTM zone the accuracy stays above 0.995 in both the *Null Island* and the *Reykjavík* scenario. What is more, for practical scenario sizes of up to 100 km (corresponding to a maximum distance to the SOP of 50 km), the accuracy in the *Null Island* and *Reykjavík* scenarios never drops below 0.999 and 0.998, respectively; for steeper thresholds of $\theta_{\text{lim}} = 25°$ in the *Null Island* scenario it even stays above 0.9999.

From this we can conclude that, for practical scenario sizes, the loss of accuracy is insubstantial, especially considering that the simulation can be expected to introduce inaccuracies in application performance at similar or larger scale (because of models that abstract away from, e.g., atmospheric effects).

VI. Proof-of-Concept Study

After discussing the theoretical benefits of a fully integrated Space-Air-Ground Integrated Network (SAGIN) simulation and the practical accuracy of the underlying Satellite Observer Position (SOP) centric approach, we now turn to a proof-of-concept simulation study to demonstrate the impact of (comparatively) small position differences of air/ground nodes in their interplay with the space segment and to investigate the efficiency of the simulation.

For investigating efficiency, we simulate 12 h of satellite mobility for the full aforementioned IRIDIUM NEXT constellation with a position update interval of 1 s.

On a mid-range Intel Core i5-10500 @ 3.1 GHz system, such a simulation performing mainly satellite mobility and coordinate transformation takes approx. 20.5 s to complete, underlining the efficiency of the fully integrated approach.

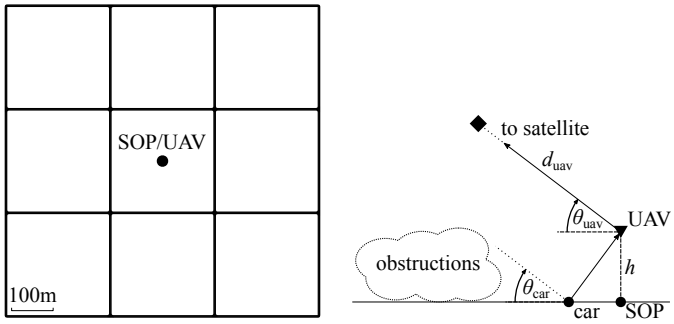

(a) top view (3×3 grid) (b) side view

Figure 10. Scenario of the proof-of-concept study in (a) top view and (b) side view. A vehicle is driving on a 3×3 Manhattan grid. It tries to communicate with a satellite via an Unmanned Aerial Vehicle (UAV) in the middle of the scenario – subject to θ_{car} or θ_{uav}, respectively, remaining below a height-dependent $\theta_{\text{lim}}(h)$.

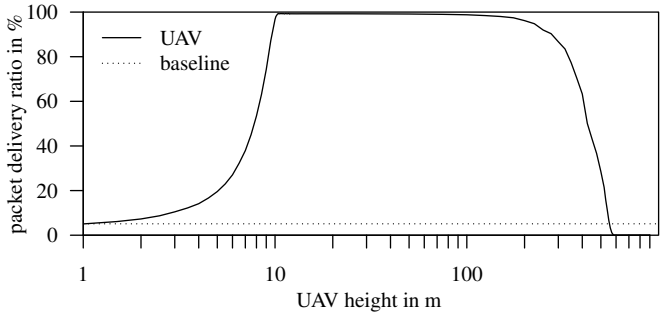

Figure 11. Packet Delivery Ratio (PDR) of a transmission from road vehicle to Low Earth Orbit (LEO) satellite constellation, optionally via an Unmanned Aerial Vehicle (UAV), as a function of the UAV height.

For the connectivity study, we consider a vehicle driving random routes on a three by three Manhattan grid with road segments of approx. 250 m each, as shown in Figure 10a. A UAV is flying at a pre-configured height in the middle of the scenario. The vehicle tries to communicate with the simulated satellites either directly or via the UAV.

We implement a very simple radio obstruction model for the V2S link: An air/ground node at a given height h can only communicate with a satellite if the elevation angle θ calculated for its relative position exceeds a height-dependent threshold, $\theta_{\text{lim}}(h)$ (see Figure 10b). To obtain plausible numbers for this simple approximation we assume obstructions up to a height of 12 m from the ground as well as a distance of 6 m between an air/ground node and the closest obstruction, so configure $\theta_{\text{lim}}(0\,\text{m}) = \arctan(12\,\text{m}/6\,\text{m}) \approx 63°$ and $\theta_{\text{lim}}(12\,\text{m}) = 0°$. For ease of illustration, we linearly interpolate in-between these bounds – a geometrically-correct channel model is beyond the scope of this proof-of-concept study and would need not just θ_{lim} to depend on azimuth angle and distance as well, but also to cater to partially obstructed Fresnel zones.

The Vehicle-to-UAV (V2U) link is modeled using the INET Framework implementation of an *outside the context of a BSS* (OCB) mode Wireless LAN link using a transmit power of 50 mW at 5.89 GHz with a receiver sensitivity of −98 dBm [33]. Channel bandwidth is set to 10 MHz, the data rate to 6 Mbit/s.

Figure 11 shows the results of this simulation study. As a result of the comparatively steep θ required for communication from the ground, the Packet Delivery Ratio (PDR) of direct V2S communication is 5 %. Enabling UAV relaying and steadily increasing UAV altitude steadily increases the PDR of the vehicle-to-UAV-to-satellite network from 5 % up to 99 % as more and more satellites come into view. This effect is only limited by a deterioration of the V2U channel as the distance between vehicle and UAV increases: For the chosen parameters the PDR already decreases noticeably at 250 m, to 92 %, and it continues to drop to zero as the UAV climbs.

We can thus conclude that (for the given scenario, which emphasizes channel effects of radio obstructions) performing fully integrated SAGIN simulation in a single, Cartesian coordinate system can successfully demonstrate the effect of comparatively small changes in the position of an air/ground node having a large impact on system performance.

VII. Conclusion and Future Work

Future Space-Air-Ground Integrated Networks (SAGINs) involving Low Earth Orbit (LEO) satellites are characterized by a high degree of mobility in all of the space, the air, and the ground segment – leading to high in-segment (and between-segment) network topology dynamics. Current surveys on SAGINs and SAGIN simulation therefore point to mobility simulation in an integrated space and ground simulation model as one of the key challenges of future research.

In this paper we demonstrated that such an integration can be achieved by using a Satellite Observer Position (SOP) centric approach to SAGIN simulation where all participants share a Cartesian coordinate system and vehicles drive on an East-North-Up (ENU) plane that is tangential to Earth at the SOP.

This approach offers the benefits of being able to work in all-Cartesian coordinates and of closely preserving the measures most relevant to modeling channels between LEO satellites and air/ground nodes. Additionally, it ensures that major directions (east, north, up) are aligned with the axes of the coordinate system (meaning, e.g., horizontal movement of vehicles and Unmanned Aerial Vehicles (UAVs) occurs strictly on a plane and buildings go straight up), also easing model implementation and efficiency.

We investigated the accuracy of this approach and found that it introduces negligible error in the calculation of the distance d between LEO satellites and air/ground nodes. What is more, while it introduces some error in the calculation of elevation angle θ at large scenario sizes (beyond approx. 100 km), this error is still small enough to be negligible for most practical purposes: We calculated worst case accuracies of 0.995 for scenarios the size of a full Universal Transverse Mercator (UTM) zone at both low and high latitudes – and worst case accuracies of 0.999 and 0.9999 (depending on θ_{lim}) for up to 100 km wide scenarios at the equator.

Finally, we demonstrated the potential of the proposed approach via a simulation of a small proof-of-concept study investigating the impact of small position differences of air/ground nodes in their interplay with the space segment in a scenario which emphasizes channel effects of radio obstructions. Based on its outcome we conclude that concepts like LEO satellite connected highly mobile nodes require novel system designs. These designs should exploit *4D topology* information (in terms of 3D topology information plus topology dynamics information) and obstacle information in order to handle handovers between air/ground nodes and LEO satellites.

We believe that the proposed approach paves the way toward fully integrated and large-scale SAGIN simulation studies employing accurate channel and macro/microscopic mobility models in all three segments – space, air, and ground – together and at scale.

ACKNOWLEDGMENTS

The authors gratefully acknowledge the help of the Luxembourg Institute of Science and Technology (LIST) with debugging and testing efforts in the context of the joint call project LEONE (Low-Latency Command and Control via LEO Satellites), supported by the Luxembourg National Research Fund (FNR) under grant IS/17800623.

REFERENCES

[1] F. Tang, C. Wen, X. Chen, and N. Kato, "Federated Learning for Intelligent Transmission with Space-Air-Ground Integrated Network toward 6G," *IEEE Network*, vol. 37, no. 2, pp. 198–204, Mar. 2023.

[2] H. Li, D. Shi, W. Wang, D. Liao, T. R. Gadekallu, and K. Yu, "Secure routing for LEO satellite network survivability," *Elsevier Computer Networks*, vol. 211, p. 109 011, Jul. 2022.

[3] H. Cui et al., "Space-air-ground integrated network (SAGIN) for 6G: Requirements, architecture and challenges," *IEEE China Communications*, vol. 19, no. 2, pp. 90–108, Feb. 2022.

[4] W. Jiang, Y. Zhan, X. Xiao, and G. Sha, "Network Simulators for Satellite-Terrestrial Integrated Networks: A Survey," *IEEE Access*, vol. 11, pp. 98 269–98 292, Sep. 2023.

[5] P. Zhang, Y. Zhang, N. Kumar, and M. Guizani, "Dynamic SFC Embedding Algorithm Assisted by Federated Learning in Space–Air–Ground-Integrated Network Resource Allocation Scenario," *IEEE Internet of Things Journal*, vol. 10, no. 11, pp. 9308–9318, Jun. 2023.

[6] J. A. Fraire, P. Madoery, F. Raverta, J. M. Finochietto, and R. Velazco, "DtnSim: Bridging the Gap Between Simulation and Implementation of Space-Terrestrial DTNs," in *6th International Conference on Space Mission Challenges for Information Technology (SMC-IT 2017)*, Madrid, Spain: IEEE, Sep. 2017.

[7] Z. Song et al., "Cooperative Satellite-Aerial-Terrestrial Systems: A Stochastic Geometry Model," *IEEE Transactions on Wireless Communications*, vol. 22, no. 1, pp. 220–236, Jan. 2023.

[8] J. Xu, M. A. Kishk, and M.-S. Alouini, "Space-Air-Ground-Sea Integrated Networks: Modeling and Coverage Analysis," *IEEE Transactions on Wireless Communications*, vol. 22, no. 9, pp. 6298–6313, Sep. 2023.

[9] B. Kloiber, T. Strang, H. Spijker, and G. Heijenk, "Improving Information Dissemination in Sparse Vehicular Networks by Adding Satellite Communication," in *2012 IEEE Intelligent Vehicles Symposium*, Alcala de Henares, Spain: IEEE, Jun. 2012, pp. 611–617.

[10] J. Puttonen, S. Rantanen, F. Laakso, J. Kurjenniemi, K. Aho, and G. Acar, "Satellite Model for Network Simulator 3," in *7th ICST International Conference on Simulation Tools and Techniques (SIMUTOOLS 2014)*, Lisbon, Portugal: ICST, Aug. 2014.

[11] A. Petrosino, G. Sciddurlo, S. Martiradonna, D. Striccoli, G. Piro, and G. Boggia, "WIP: An Open-Source Tool for Evaluating System-Level Performance of NB-IoT Non-Terrestrial Networks," in *22nd IEEE International Symposium on a World of Wireless, Mobile and Multimedia Networks (WoWMoM 2021)*, Pisa, Italy: IEEE, Jun. 2021.

[12] J. A. Fraire, P. Madoery, M. A. Mesbah, O. Iova, and F. Valois, "Simulating LoRa-Based Direct-to-Satellite IoT Networks with FLORASAT," in *23rd IEEE International Symposium on a World of Wireless, Mobile and Multimedia Networks (WoWMoM 2022)*, Belfast, UK: IEEE, Jun. 2022.

[13] X. Wang, X. Chen, H. Ye, Y. Liu, and G. Zhang, "Cloud-Based Experimental Platform for the Space-Ground Integrated Network," *Wiley/Hindawi Wireless Communications and Mobile Computing*, Oct. 2020.

[14] S. Kassing, D. Bhattacherjee, A. B. Águas, J. E. Saethre, and A. Singla, "Exploring the "Internet from space" with Hypatia," in *ACM Internet Measurement Conference (IMC 2020)*, Virtual Conference: ACM, Oct. 2020.

[15] T. Schubert, L. Wolf, and U. Kulau, "ns-3-leo: Evaluation Tool for Satellite Swarm Communication Protocols," *IEEE Access*, vol. 10, pp. 11 527–11 537, Jan. 2022.

[16] A. Freimann, M. Dierkes, T. Petermann, C. Liman, F. Kempf, and K. Schilling, "ESTNeT: a discrete event simulator for space-terrestrial networks," *CEAS Space Journal*, vol. 13, no. 1, pp. 39–49, May 2020.

[17] T. Pfandzelter and D. Bermbach, "Celestial: Virtual Software System Testbeds for the LEO Edge," in *23rd ACM/IFIP International Middleware Conference*, Québec City, Québec, Canada: ACM, Nov. 2022, pp. 69–81.

[18] A. Valentine and G. Parisis, "Developing and Experimenting with LEO Satellite Constellations in OMNeT++," in *8th OMNeT++ Community Summit (OMNeT++ 2021)*, Virtual Conference, Sep. 2021.

[19] B. Kempton and A. Riedl, "Network Simulator for Large Low Earth Orbit Satellite Networks," in *IEEE International Conference on Communications (ICC 2021)*, Virtual Conference / Montreal, Canada: IEEE, Jun. 2021.

[20] J. Puttonen, L. Sormunen, H. Martikainen, S. Rantanen, and J. Kurjenniemi, "A System Simulator for 5G Non-Terrestrial Network Evaluations," in *22nd IEEE International Symposium on a World of Wireless, Mobile and Multimedia Networks (WoWMoM 2021)*, Pisa, Italy: IEEE, Jun. 2021.

[21] N. Cheng et al., "A Comprehensive Simulation Platform for Space-Air-Ground Integrated Network," *IEEE Wireless Communications*, vol. 27, no. 1, pp. 178–185, Feb. 2020.

[22] M. Franke, F. Klingler, and C. Sommer, "Poster: Simulating Hybrid LEO Satellite and V2X Networks," in *13th IEEE Vehicular Networking Conference (VNC 2021), Poster Session*, Virtual Conference: IEEE, Nov. 2021, pp. 139–140.

[23] C. Sommer, R. German, and F. Dressler, "Bidirectionally Coupled Network and Road Traffic Simulation for Improved IVC Analysis," *IEEE Transactions on Mobile Computing*, vol. 10, no. 1, pp. 3–15, Jan. 2011.

[24] L. Mészáros, A. Varga, and M. Kirsche, "INET Framework," in *Recent Advances in Network Simulation*, A. Virdis and M. Kirsche, Eds. Springer, 2019, pp. 55–106.

[25] A. Varga and R. Hornig, "An Overview of the OMNeT++ Simulation Environment," in *1st International ICST Conference on Simulation Tools and Techniques for Communications, Networks and Systems (SIMUTOOLS 2008)*, Marseille, France: ICST, 2008.

[26] P. A. Lopez et al., "Microscopic Traffic Simulation using SUMO," in *2018 21st International Conference on Intelligent Transportation Systems (ITSC)*, IEEE, Nov. 2018, pp. 2575–2582.

[27] "Measurement techniques and new technologies for satellite monitoring," ITU, Report ITU-R SM.2424-0, Jun. 2018.

[28] D. A. Vallado and P. J. Cefola, "Two-line Element Sets - Practice and Use," in *63rd International Astronautical Congress (IAC)*, International Astronautical Federation, Oct. 2012.

[29] D. Vallado, P. Crawford, R. Hujsak, and T. S. Kelso, "Revisiting Spacetrack Report #3 (AIAA 2006-6753)," in *AIAA/AAS Astrodynamics Specialist Conference and Exhibit*, Keystone, CO: AIAA, Aug. 2006.

[30] "Order and Authorization 22-91," Federal Communications Commission (FCC), DA/FCC 22-91, Dec. 2022, pp. 1–74.

[31] B. Rhodes, *Skyfield: High precision research-grade positions for planets and Earth satellites generator*, Astrophysics Source Code Library, record ascl:1907.024, Jul. 2019.

[32] C. Sommer et al., "Veins – the open source vehicular network simulation framework," in *Recent Advances in Network Simulation*, A. Virdis and M. Kirsche, Eds., Springer, 2019, pp. 215–252.

[33] B. Bloessl and A. O'Driscoll, "A Case for Good Defaults: Pitfalls in VANET Physical Layer Simulations," in *2019 Wireless Days (WD)*, IEEE, Apr. 2019.